Applied Thermal Engineering 59 (2013) 370–379

Contents lists available at SciVerse ScienceDirect

Applied Thermal Engineering

journal homepage: www.elsevier.com/locate/apthermeng

Analysis of a membrane based air-dehumidification unit for air conditioning in tropical climates

Khin Zaw [a,*], M. Reza Safizadeh [a,c], Joachim Luther [a], Kim Choon Ng [b]

[a] Solar Energy Research Institute of Singapore (SERIS), 7 Engineering Drive 1, Block E3A, #06-01, Singapore 117574, Singapore
[b] Department of Mechanical Engineering, National University of Singapore (NUS), Singapore
[c] NUS Graduate School for Integrative Science & Engineering, National University of Singapore, Singapore

HIGHLIGHTS

- A simple cross-flow membrane based air-dehumidification unit is analysed for tropics.
- Experiments, physical modeling and computer simulations have been performed for the analyses of a laboratory type dehumidification unit.
- A moisture reduction of up to 8 g per kg of dry air for humid ambient air having a moisture content of 20 g per kg of dry air while the air flow rate is of 20 m^3/h.
- Results show the membrane based dehumidification is driven by vapor pressure gradient between incoming ambient air and the relatively dry exhaust air from a building.
- No electricity consumption for the process except for air transport.

ARTICLE INFO

Article history:
Received 22 December 2012
Accepted 17 May 2013
Available online 31 May 2013

Keywords:
Air dehumidification
Membrane technology
Air-conditioning
Tropical regions

ABSTRACT

The dehumidification potential of a cross-flow membrane based air-dehumidification unit is analysed for tropical climatic conditions. The process of dehumidification is driven by the gradient of the concentration of water vapour between the incoming ambient air and the relatively dry exhaust air from a building. Electric energy is used for air transport only. This paper reports on experiments, physical modelling and computer simulations performed for the analysis of a laboratory-type dehumidification unit in Singapore. Experimentally moisture reductions between 4 g and 8 g of moisture per kg of moist air have been achieved for high humidity ambient air conditions (16 g/kg and 20 g/kg, respectively). Membrane dehumidification units may be used as stand-alone dehumidification units or as pre-dehumidification devices in the context of more complex air-conditioning systems in tropical climates.

1. Introduction

Worldwide application of air-conditioning systems in residential, industrial and commercial buildings is increasing significantly, leading to a growing electricity demand. Conventional air cooling machines handle both air dehumidification (latent loads) and air cooling (sensible loads) simultaneously in an electric energy-intensive manner. In particular in tropical regions, electricity consumption will be high because of the large amount of latent load. Separate handling of latent and sensible loads using different components may be advantageous as the air dehumidification process can be effectively done by electricity efficient techniques, e.g., membrane, absorption and desiccant adsorption technologies driven by heat energy [1–5].

This paper focuses on the analysis of a laboratory-type membrane dehumidification unit that offers an electricity efficient way of air dehumidification. In general, air dehumidification has to be followed by a separate cooling step of the dehumidified air (sensible cooling). Membrane technology is a powerful method for the energy efficient separation of substances. Membrane separation technologies are widely applied in areas like food processing, water treatment, electrochemistry, etc. [6–11]. A plethora of research has been done on the analysis and the development of such technologies. The application of membrane technologies to air dehumidification in electricity efficient air-conditioning systems has gained importance during the last decade. Zhang et al. [12–15] conducted in-depth theoretical and experimental analyses of membrane based mass and heat transfer processes using different membrane materials and different physical configuration of membrane units. Scovazzo et al. [16], investigated membrane based humidity control methods using different types of membranes. Some research

* Corresponding author. Tel.: +65 8322 8457.
E-mail address: mkhinzaw@gmail.com (K. Zaw).

1359-4311/$ – see front matter © 2013 Elsevier Ltd. All rights reserved.
http://dx.doi.org/10.1016/j.applthermaleng.2013.05.029

groups focused on the optimization of membrane structures for air dehumidification applications [e.g. Refs. [17,18]]. These analyses point out that the membrane based mass and heat transfer could be fruitfully utilized for air dehumidification in air-conditioning systems. However, many challenges are still remaining to improve membrane technologies for moisture and heat transfer processes. In particular a lack of membrane based air-dehumidification research for tropical climates is found. Additionally, the primary advantages of membrane based technologies such as low initial investment, energy efficiency, simplicity of operation and low operation cost encourage us to evaluate the potential application of membrane technology in tropical regions. This work is focussing on a membrane based air dehumidification system for the tropics.

In this paper, we report on experimental and theoretical simulations (using COMSOL software) of a laboratory-type membrane based air-dehumidification research unit operated under Singapore climate. For simplicity, the unit is designed as an air-to-air cross flow moisture and heat exchanger. The driving force of the air-dehumidification is the gradient of the concentration of water vapour between the incoming ambient supply air (high humid air) and the relatively dry exhaust air from an air-conditioned room. Except for air transportation, no electric energy is used in this configuration.

2. Experimental set up of membrane moisture exchanger

The principle of a membrane based moisture and heat exchanger is shown in Fig. 1. A humid primary air stream and a relatively dry secondary air stream enter the unit on either side of a membrane layer. The moisture permeation takes place between the primary air and secondary air through the membrane.

An experimental test facility for the experimental analysis of a cross-flow membrane moisture exchanger unit integrating variable speed controlled fans and a humidity control chamber (see Fig. 2) was installed in a laboratory of the Solar Energy Research Institute of Singapore (SERIS). The membrane unit is composed of 40 pieces of frames (see Fig. 3) made of the Bakelite material with the thermal conductivity of 0.23 W/(m K). A fibre-type membrane sheet from a membrane unit (ZehnderComfoAir 350) as shown in Fig. 4 was fastened with glue on each side of the frame. The Bakelite frames with the membrane layers were then assembled together to form the cross-flow membrane unit. The detailed information of the cross-flow membrane moisture exchanger is given in Table 1. A humidity control chamber was designed and fabricated in order to control and maintain the moisture content of the primary air stream during the experiments. This chamber simulates primary air streams with different moisture contents. The secondary air stream is taken from an air conditioned space. Steady state conditions of the air streams were maintained. During the experiments, the relative humidity (RH), temperature and air flow rates of various air

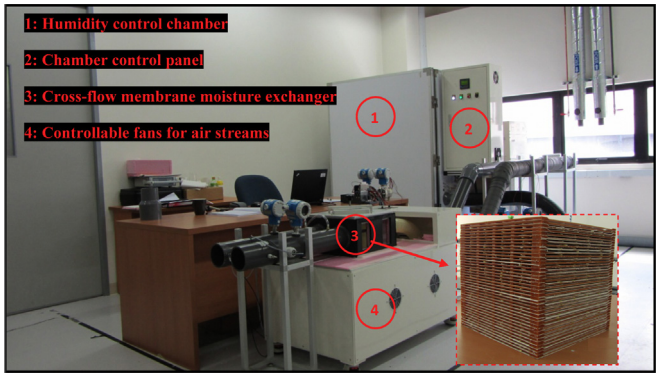

Fig. 2. Experimental set up for the analysis of membrane based air dehumidification systems. The primary air (ambient air) is simulated using the humidity control chamber (1). The secondary air is taken from an air conditioned room. The primary and secondary air streams can be adjusted using the controllable fans in subsystem 4, and the two air streams are sent into the membrane moisture exchanger unit (3).

streams were measured. The specifications of the applied sensors are listed in Table 2. In order to reduce the systematic error in experiments, the air temperature was measured by 4-wire RTD temperature sensor. The RH sensors reading were checked with a

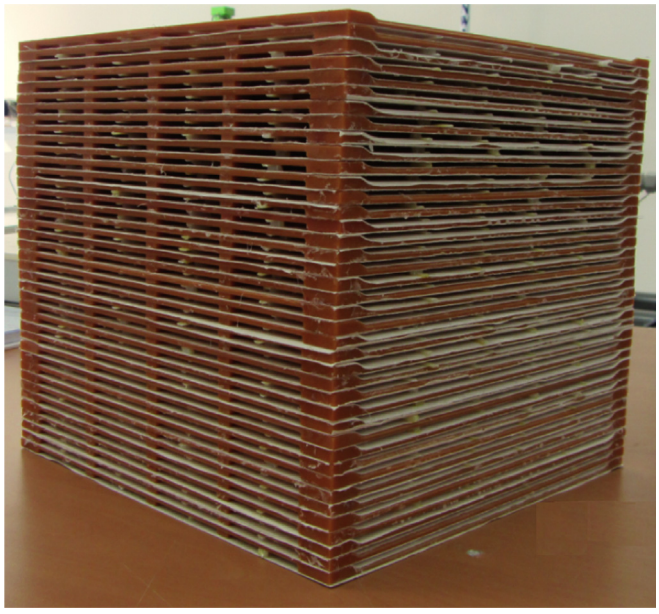

Fig. 3. Membrane based moisture exchange unit ($L \times W \times H$: 17 cm × 17 cm × 19 cm). The height includes the thickness of the frames, membrane papers and glue.

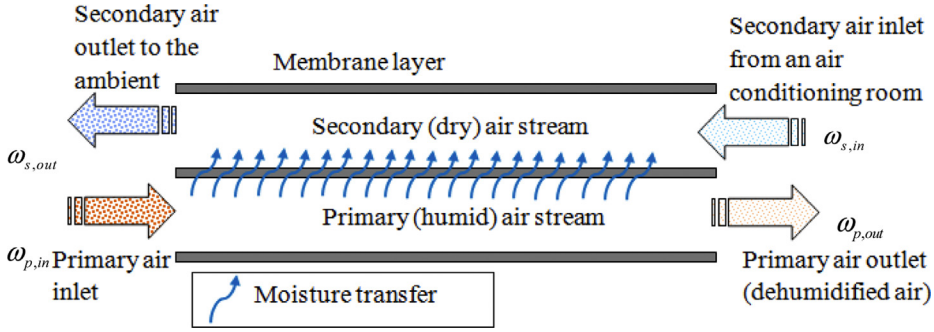

Fig. 1. Principle of a membrane based moisture and heat exchanger. The ω characterizes the humidity ratio of the corresponding air flows (a counter flow diagram is shown in this figure; in the experiments a cross flow scheme was applied, see Fig. 5).

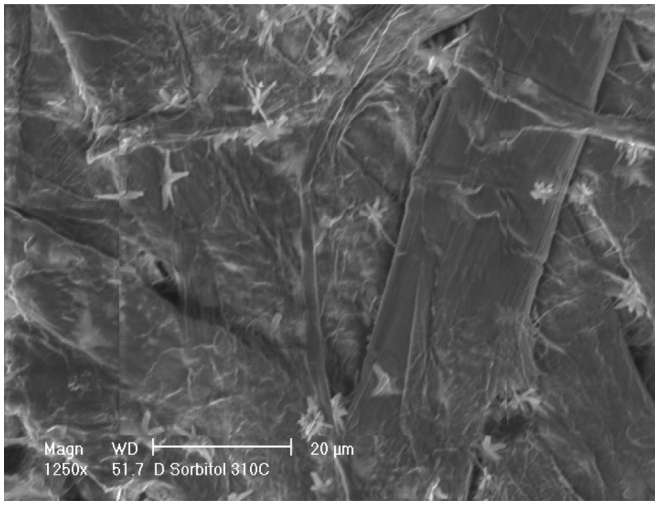

Fig. 4. Scanning Electron Microscope (SEM) picture of the membrane material used in the experiments. (Legend illustrates actual width 20 µm on the SEM picture).

Table 1
Parameters of the membrane moisture exchange unit.

	Value	Unit
Length of supporting frame	170	mm
Width of supporting frame	170	mm
Area of each membrane barrier	0.03	m^2
Number of membranes	80	–
Total supporting frames	40	–
Total area of membranes	2.31	m^2
Number of primary air channels	40	–
Number of Secondary air channels	40	–
Height of each air channel	2	mm

master optical dew-point meter with high accuracy, high resolution and virtually zero drift (Michell-Optidew Vision). The relative humidity values from RH sensors and dew-point meter sensors at constant temperature (23 °C) and several relative humidity (25%, 50% and 80%) were always within ±2%. The humidity ratios of the air streams (the amount of water vapour content in grams in a kilogram of dry air) were calculated by using measured values, and psychometric models [19] while the air pressure was assumed at 1 atm. Due to the steady state condition of the air streams, it was sufficient to record the data every 60 s. For the analyses explained below the data acquired were averaged subsequently.

3. Mathematical modelling

A numerical simulation model of the membrane-based moisture exchanger described in this paper has been developed. The assumptions for modelling are as follows:

(i) The moisture transfer process can be described by transport and diffusion equations.
(ii) A steady state equilibrium model is applicable.
(iii) Air velocities of the primary and secondary air streams remain constant throughout the primary and secondary air channels. No air flows inside the membrane layer.
(iv) The fluid flow is laminar, steady, incompressible and hydrodynamically developed.
(v) Moisture from the primary air stream passes through the membrane to the secondary air stream in normal direction to the membrane plan.
(vi) The water vapour concentration of the air in the primary, the secondary channels and the membrane varies in x, y and z directions.
(vii) (For simplicity) no heat transfer is considered between the two air streams.

As shown in Fig. 5, the three dimensional modelling was done using three adjacent spatial domains in z-direction: the flow channel of the primary air, the membrane layer and the secondary air flow channel. These three domains are interconnected to each other. During the moisture permeation process, the moisture from the primary air is firstly adsorbed onto the surface of the membrane adjacent to the primary channel, secondly transported through the membrane to the other surface of the membrane and finally desorbed into the secondary air stream. The steady state mathematical sub-models for moisture conservation in the two channels and for mass transport through the membrane are presented in the following.

3.1. Primary air channel

The water concentration in the primary air channel is modelled on the basis of a gas convection–diffusion model, in combination with the moisture transport from the primary air to the membrane [20].

$$\mathbf{u}_{\mathrm{p}}(y)\frac{\partial c_{\mathrm{p}}(x,y,z)}{\partial y} = D_{\mathrm{p}}\left(\frac{\partial^2 c_p(x,y,z)}{\partial x^2}+\frac{\partial^2 c_{\mathrm{p}}(x,y,z)}{\partial y^2}+\frac{\partial^2 c_{\mathrm{p}}(x,y,z)}{\partial z^2}\right) - S_{\mathrm{sink}}(x,y) \tag{1}$$

where c_{p}, D_{p}, $\mathbf{u}_{\mathrm{p}}$, and S_{sink} are water concentration in the primary air kg/m^3, diffusion coefficient of water vapour in the primary air in m^2/s, air velocity in the primary air channel in m/s, and specific moisture flux rate from the primary air to the membrane's surface in kg/m^2 s.

3.2. The interface between the primary air channel and the membrane

The mass transfer between the primary air and the membrane surface adjacent to the primary channel is driven by the water concentration difference between the primary air and the membrane surface. The local specific moisture flux rate across the surface of the membrane is then given by:

Table 2
Specification of measuring instruments.

Instrument/sensor	Measuring range	Accuracy	Manufacturer
Temperature	−50 to 100 °C	1/10 DIN (0.03 °C at 0 °C)	Omega
Relative humidity	0–100%	±2% (10–90%) at 23 °C humidity	Michel
Absolute pressure	0–2 bar	0.075%	Endress and Hausers
Differential pressure	0–1000 Pa	0.075%	Endress and Hausers
Air flow meter	0–513 m^3/h	1% of measured air volume	Endress and Hausers

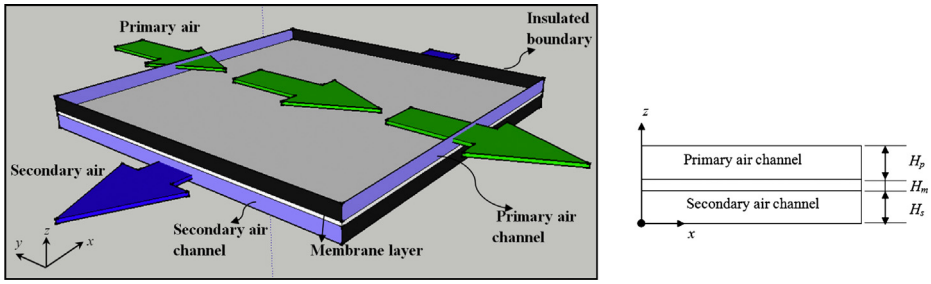

Fig. 5. Schematic drawing of the cross-flow membrane based moisture exchanger. Three spatial domains in z-directions are applied for the physical simulation of the system: the primary air channel, the secondary air channel and the membrane layer. The primary air (green arrow) and the secondary air (blue arrow) are flowing above and below of the membrane layer (shown in white colour). The cross section at the right side shows the dimension in z-direction and it is the surface of the membrane unit where the primary air comes out after passing through the membrane unit. (For interpretation of the references to colour in this figure legend, the reader is referred to the web version of this article.)

$$S_{\text{sink}}(x,y) = -D_{\text{m}}\frac{\partial c_{\text{m}}(x,y,z)}{\partial z}\bigg|_{z=H_{\text{s}}+H_{\text{m}}} = -k_{\text{p}}\left(c_{\text{m}}(x,y,z) - c_{\text{p}}(x,y,z)\right)\big|_{z=H_{\text{s}}+H_{\text{m}}} \quad (2)$$

where c_{m} is the water concentration at the surface of membrane, D_{m} is water diffusion coefficient of the membrane in m^2/s, k_{p} is the mass transfer coefficient (m/s) describing the moisture transfer between the primary air and the surface of the membrane in the primary channel, and H_{s} and H_{m} are the height of primary channel and thickness of membrane, respectively.

3.3. Membrane

The moisture diffusion process through the membrane is characterized by mass conservation. Due to the cross-flow configuration of the membrane unit, the water concentration of membrane varies besides in z and also in x and y. Since the water vapour velocity inside the membrane is very low, the right side of Eq. (3) is assumed to be zero.

$$-D_{\text{m}}\left(\frac{\partial^2 c_{\text{m}}}{\partial x^2} + \frac{\partial^2 c_{\text{m}}}{\partial y^2} + \frac{\partial^2 c_{\text{m}}}{\partial z^2}\right) = 0 \quad (3)$$

3.4. The interface between the membrane and the secondary air channel

At the boundary of the membrane and the secondary air stream, the moisture transport from the membrane surface to the relatively dry air in the secondary channel is driven by the water concentration difference between the membrane's surface and the secondary air. The equation below presents the specific moisture flux rate from the membrane to the air in the secondary channel.

$$S_{\text{source}}(x,y) = -D_{\text{m}}\frac{\partial c_{\text{m}}(x,y,z)}{\partial z}\bigg|_{z=H_{\text{s}}} = -k_{\text{s}}(c_{\text{s}}(x,y,z) - c_{\text{m}}(x,y,z))|_{z=H_{\text{s}}} \quad (4)$$

where S_{source} is the specific moisture flux rate from the membrane's surface to the secondary air in kg/m^2 s, k_{s} is the mass transfer coefficient (m/s) describing the moisture transfer between the surface of the membrane and the secondary air, c_{s} is the water concentration of the secondary air in kg/m^3, and H_{s} is the height of secondary channel.

3.5. The secondary air channel

The moisture concentration inside the secondary air channel is modelled as

$$\mathbf{u}_{\text{s}}(x)\frac{\partial c_{\text{s}}(x,y,z)}{\partial x} = D_{\text{s}}\left(\frac{\partial^2 c_{\text{s}}(x,y,z)}{\partial x^2} + \frac{\partial^2 c_{\text{s}}(x,y,z)}{\partial y^2} + \frac{\partial^2 c_{\text{s}}(x,y,z)}{\partial z^2}\right) + S_{\text{source}}(x,y) \quad (5)$$

where $\mathbf{u}_{\text{s}}$ is the air velocity of the secondary air stream, D_{s} is the moisture diffusivity in the secondary air, and S_{source} is defined in Eq (4).

3.6. Parameters

In the mathematical modelling, the diffusion coefficients D_{p} and D_{s} are a function on the primary and secondary air temperature [21]. The diffusion coefficient of the membrane D_{m} is determined by comparing experimental data and the results from simulation calculations (see Section 4.2). The mass transfer coefficients k_{p} and k_{s} (m/s) as used in Eqs. (6–9) are a function of the diffusion coefficients and the air temperature [21]:

$$k_i = \frac{\text{Sh}_i \times D_i}{L},\ i = \text{p},\text{s} \quad (6)$$

where the subscripts "p" and "s" refer to the primary and secondary air streams. Sh is Sherwood number, and is evaluated by

$$\text{Sh}_i = 0.664 \times \sqrt{\text{Re}_i} \times \sqrt[3]{\text{Sc}_i} \quad (7)$$

where *Re* is Reynolds number

$$\text{Re}_i = (\rho_i u_i L)/\mu_i,\ i = \text{p},\text{s} \quad (8)$$

And Sc is Schmidt number, respectively

$$\text{Sc}_i = \mu_i/(\rho_i D_i),\ i = \text{p},\text{s} \quad (9)$$

In Eqs. (6–9), ρ_i denotes the density in kg/m^3, u_i represents the air velocity in m/s, μ_i is the dynamic viscosity of the air in kg/(m s) and L is the characteristic length [22] in metre of the air channel, respectively.

3.7. Parameters and boundary conditions

In our model, the primary and secondary air velocities ($\mathbf{u}_{\text{p}}$ and $\mathbf{u}_{\text{s}}$), and the moisture concentration at the primary and secondary air inlet (c_{p} and c_{s}) are input parameters to the model. c_{p} and c_{s} can be calculated as:

$$c = \rho\omega \quad (10)$$

where ρ is the density of air and ω is humidity ratio of the air. It is assumed that water transport by diffusion can be neglected at the

outlet of the air channels. This applies to the outlet boundary of the primary air domain (x–z plane at $y = 0$, see Fig. 5) and the outlet boundary of the secondary air domain (y–z plane at $x = 0$).

The above given system of coupled differential equations was solved using the commercial Finite Element Analysis (FEA) [23] software, COMSOL (3.5.a). The numerical analysis provided the water vapour concentration values in the primary and secondary air channels and in particular – for comparison with the experiments – the water vapour concentration at the outlet of these channels.

4. Results

4.1. Experimental analyses

Experiments were conducted for volumetric air flows in the range of [20, 80] m^3/h for both primary and secondary air. The experimental results – the humidity ratios of the primary air inlet $\omega_{p,in}$, primary air outlet (after passing the membrane dehumidification unit) $\omega_{p,out}$ and the secondary air inlet from an air conditioning room $\omega_{s,in}$ – at air flow rates of 20 m^3/h and 80 m^3/h are shown in Fig. 6. The data in Fig. 6 correspond to different experiments. At conditions of $\omega_{p,in}$ of about 20 g/kg and $\omega_{s,in}$ of about 7–8 g/kg, the experimental results show a humidity ratio of the dehumidified air $\omega_{p,out}$of about 12 g/kg at an air flow rate of 20 m^3/h and about 15 g/kg at 80 m^3/h, respectively. This indicates that the dehumidification performance of the membrane unit is highly dependent on two parameters – the air flow rate through the membrane unit and the water vapour gradient between the two air streams. In order to analyse this in a quantitative way parametric analyses have been performed.

As a measure of the performance of the dehumidification unit the latent effectiveness η is defined as [24]

$$\eta = \frac{(\omega_{p,in} - \omega_{p,out})}{(\omega_{p,in} - \omega_{s,in})}, \tag{11}$$

where $\omega_{p,in}$, $\omega_{p,out}$, and $\omega_{s,in}$ are the humidity ratio in g/kg of the primary air inlet, that of the primary air outlet and that of the secondary air inlet of the membrane moisture exchanger (see Fig. 1). The maximum dehumidification potential is given by ω^P.

$$\omega^P = \omega_{p,in} - \omega_{s,in} \tag{12}$$

In order to allow for an extrapolation of the experimental results, a specific air flow rate ν is defined as follow:

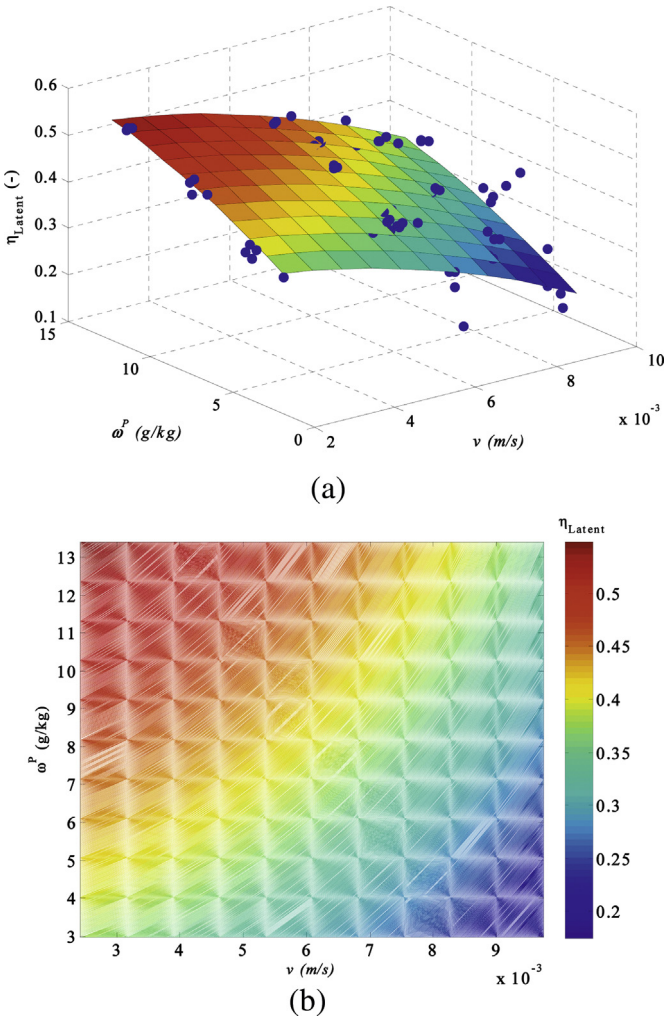

Fig. 7. Latent effectiveness (Eq. (11)) as a function of specific air flow and dehumidification potential: (a) three dimensional mesh generated by a least square curve fitting method using experimental data (blue dots), and (b) the equivalent contour plot. (For interpretation of the references to colour in this figure legend, the reader is referred to the web version of this article.)

$$\nu = \frac{\text{Volumetric air flow rate in } m^3/s}{\text{total area of the membrane in } m^2} = \frac{\dot{V}}{A} \tag{13}$$

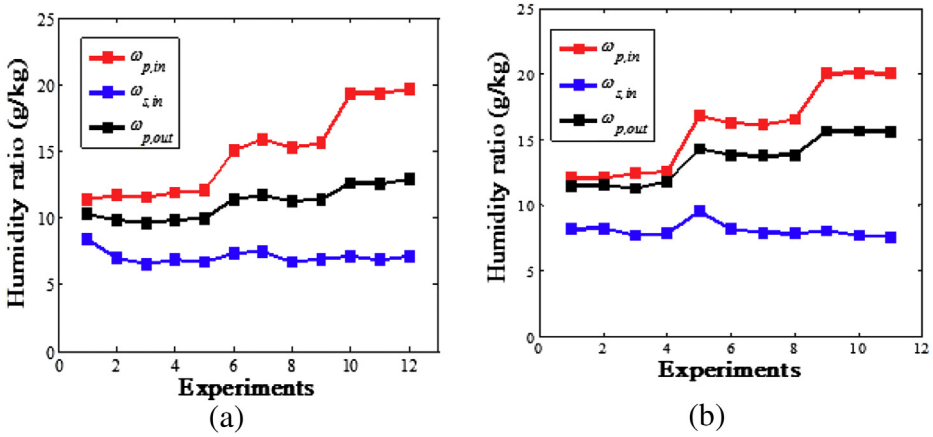

Fig. 6. Humidity ratios of the primary air inlet $\omega_{p,in}$, the primary air outlet (after passing through the membrane unit) $\omega_{p,out}$ and the secondary air inlet $\omega_{s,in}$at (a) the air flow rate of 20 m^3/h and (b) the air flow rate of 80 m^3/h, for different experiments performed.

Table 3
Primary/moist air and secondary dry air conditions of nine different experiments.

No.	Air flow (m^3/h)	Primary air humidity ratio (g/kg)	Secondary air humidity ratio (g/kg)	Primary air temperature (°C)	Secondary air temperature (°C)
1	50	12.1	8.4	29.7	22.5
2		16.2	7.3	29.0	24.6
3		19.8	7.2	28.6	27.5
4	70	12.9	8.3	30.0	20.5
5		16.5	7.9	30.0	24.6
6		20.1	8.1	29.5	26.5
7	80	12.4	7.7	30.1	22.4
8		16.5	7.9	30.3	24.3
9		20.1	8.1	29.6	26.3

It links the absolute flow rate to the total surface area of the membrane. A set of measured data triples represented by the latent effectiveness η, the specific air flow rate ν and the dehumidification potential ω^P, $\mathbf{S} = \{(\eta_1, \nu_1, \omega_1^P), (\eta_2, \nu_2, \omega_2^P), \ldots, (\eta_n, \nu_n, \omega_n^P)\}$, were then fitted to a second order polynomial:

$$\eta_j = \alpha_0 + \alpha_1 \nu_j + \alpha_2 \omega_j^P + \alpha_3 \nu_j^2 + \alpha_4 \left(\omega_j^P\right)^2 + \alpha_5 \nu_j \omega_j^P, \quad j = 1, 2, \ldots, n \tag{14}$$

where α_i, $i = 0,\ldots,5$ are the coefficients to be determined by the fitting procedure (least square technique [25]).

Using Eq. (14) and the data of 74 experiments (i.e., $n = 74$), the coefficients α_i were determined as $\alpha_0 = 0.32$, $\alpha_1 = -2.33$ (s/m), $\alpha_2 = 0.03$ (g/kg)$^{-1}$, $\alpha_3 = -2.09 \times 10^3$ (m/s)$^{-2}$, $\alpha_4 = -5.38 \times 10^{-4}$ (g/kg)$^{-2}$, and $\alpha_5 = 0.04$ (kg s/m g^{-1}). Given the maximum absolute values of ν_j and ω_j^P (0.01 m/s and 15 g/kg respectively in the experimental data set) it is observed that the coefficients α_5 and can be neglected for further analysis. The coefficient α_3 reflect the negative effect of an increasing specific flow rate on the latent effectiveness η while α_2 characterises the increase of η with increasing maximum dehumidification potential ω^P. The root mean square (r.m.s) error between the approximation and the measured values is 0.05. The approximation results are shown graphically in Fig. 7. Since the dehumidification potential ω^P is given by external boundary conditions the main parameter that may be varied for optimisation is the specific flow rate. Fig. 7 presents quantitative information on this fact.

In practical air conditioning applications in tropical climates, the dehumidification potential of a system based on our experimental design could range between 4 g/kg and 8 g/kg (assuming a humidity ratio of the primary ambient air of 16 g/kg and 20 g/kg respectively while a humidity ratio of the secondary air from an air conditioned room is approximately 8 g/kg and the air flow is of 20 m^3/h, see Fig. 6). Under these assumptions the latent effectiveness η would be in the range of 0.25–0.5 based on the shown quantitative information in Fig. 7.

4.2. Determination of the mass diffusion coefficient of the membrane

The mass diffusion coefficient D_m was determined by comparing the experimental data with the results of the FEA simulation calculations (see Section 3). Nine experiments which covered different operation conditions – (i) different air flow rates and (ii) different dehumidification potential – were selected for the D_m identification process. Table 3 gives the operating conditions of the primary air stream and the secondary air stream of the nine experiments.

The water diffusion coefficient of membrane is subsequently determined by minimizing the error function

$$e(D_m) = \sum_{i=1}^{9} \left(e_{p,out}(D_m) + e_{s,out}(D_m)\right), \quad D_m \in D \tag{15}$$

where D_m is the diffusion coefficient in the parameter domain D in a possible range of 0.5×10^{-6}–2.5×10^{-6} m^2/s, $e_{p,out}(D_m)$ is the absolute deviation between the computed humidity ratio (that is the averaged humidity ratio value at the outlet of the primary air stream in the x–z plane as shown in Fig. 5) and the measured humidity ratio at the outlet of the primary air stream; $e_{s,out}(D_m)$is the corresponding value for the secondary air stream. This procedure resulted in a value of $D_m = 1.5 \times 10^{-6}$ m^2/s, which is in the range of water diffusion coefficients given for air-dehumidification membranes in the literature [20]. Using the value of D_m given above, the maximum deviations in $e_{p,out}(D_m)$ and $e_{s,out}(D_m)$ are 8% for an air flow of 50 m^3/h as shown in Fig. 8, and 11% for an air flow of 80 m^3/h in Fig. 9, respectively. Using the obtained value of D_m, further simulations have been done for other experimental cases. The results of these simulations are summarized in Table 4 (as well as Tables 6 and 7). Discussions of the results are given in Section 4.4.

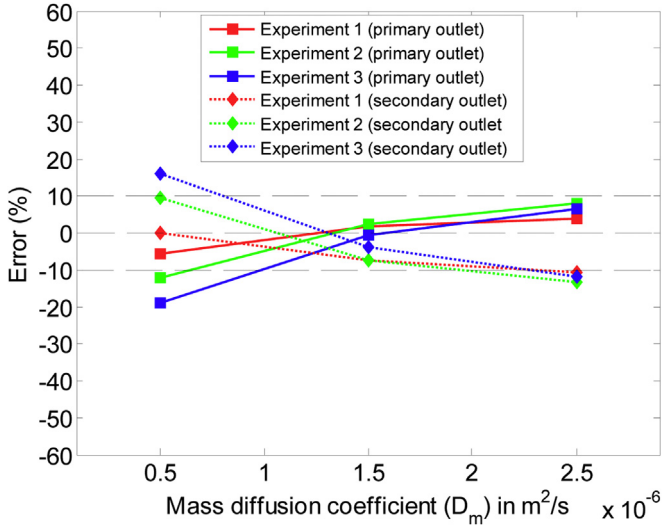

Fig. 8. Relative error between computed and measured humidity ratio values for different parameter values of the water diffusion coefficient (Air flow rate 50 m^3/h).

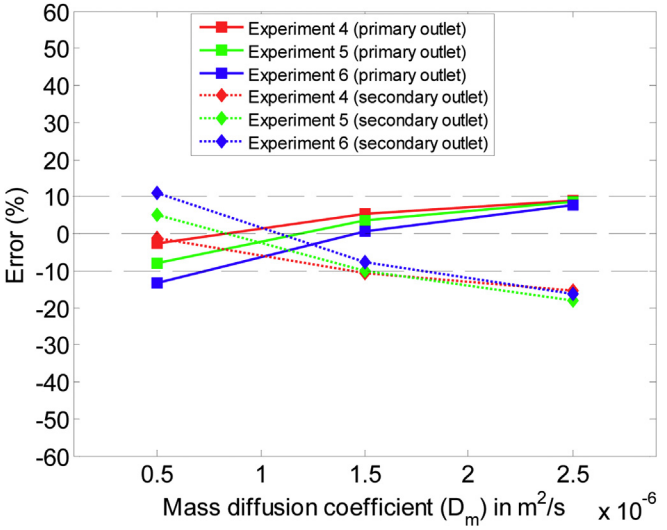

Fig. 9. Relative error between computed and measured humidity ratio values for different parameter values of the water diffusion coefficient (Air flow rate 80 m^3/h).

Table 4
Experimental and simulated humidity ratios (g/kg) of the primary air and secondary air for different experimental condition.

Exp no.	Air flow (m^3/h)	Boundary conditions		Output conditions					
		$\omega_{p,in}$ (g/kg)	$\omega_{s,in}$ (g/kg)	$\omega_{p,out}$ (g/kg)			$\omega_{s,out}$ (g/kg)		
				Exp	Sim	Error (%)	Exp	Sim	Error (%)
1	20	11.4	8.4	10.3	9.6	6.8	9.7	10.2	−5.2
2	50	19.8	8.3	13.9	14.4	−3.6	13.4	13.6	−1.5
3	60	12.2	7.4	11.0	10.2	7.3	8.7	9.4	−8.0
4	70	12.9	7.6	11.5	10.9	5.2	9.5	9.6	−1.1
5	80	12.1	8.2	11.5	10.7	7	9.1	9.5	−4.4
6	80	16.8	9.5	14.3	14.1	1.4	11.5	12.1	−5.2
7	80	20.1	8.1	15.7	15.6	0.6	11.7	12.6	−7.7

4.3. Spatially resolved water concentration in the dehumidification unit

Using the numerical value of D_m from Section 4.2, simulations have been carried out using the parameters given in Table 5. Fig. 10 depicts the simulated moisture distribution in the primary air channel and the secondary air channel for an exemplary experimental condition (inlet primary air condition of $\omega_{p,in} = 19.8$ g/kg and air temperature of 28.6 °C, inlet secondary air condition of $\omega_{s,in} = 7.2$ g/kg and air temperature of 27.5 °C). Fig. 10 demonstrates the principle of the cross-flow membrane based air dehumidification process: (i) the moisture concentration of the primary air decreases while that of the secondary air increases and (ii) the moisture concentration varies diagonally because the air streams pass in a cross-flow manner on either side of the membrane layer.

4.4. Reduction of latent loads in air conditioning applications and related electricity consumption

The reduction in water content of the primary air can be transformed into a reduction of the latent load ΔQ of the ambient supply air in air conditioning applications.

$$\Delta Q = \Delta\omega \times \dot{m} \times h, \tag{16}$$

or in terms of the specific flow rate v

$$\Delta Q = \Delta\omega \times \rho \times A \times v \times h, \tag{17}$$

where $\Delta\omega$ is the amount of moisture removed from the supply air and transferred to the secondary air, $\dot{m}$ is primary air flow rate in kg/s, h is the specific enthalpy of saturated water vapour at the given temperature of the air [19], ρ is the density of the air, and A is total surface area of membrane used in our application. ΔQ can be normalised to the "full latent load for air conditioning in Singapore" ΔQ_{SCC} as

$$\Delta\overline{Q} = \frac{\Delta Q}{\Delta Q_{SCC}} \tag{18}$$

Table 5
Parameters of primary and secondary air for the COMSOL finite element model calculations.

Description	Primary air	Secondary air
Temperature (°C)	28.6 °C	27.5 °C
Dynamic viscosity (kg m^{-1} s^{-1})	1.73×10^{-5}	1.72×10^{-5}
Air volume flow rate (m^3 h^{-1})	50	50
Humidity Ratio (g kg^{-1})	19.8	7.2

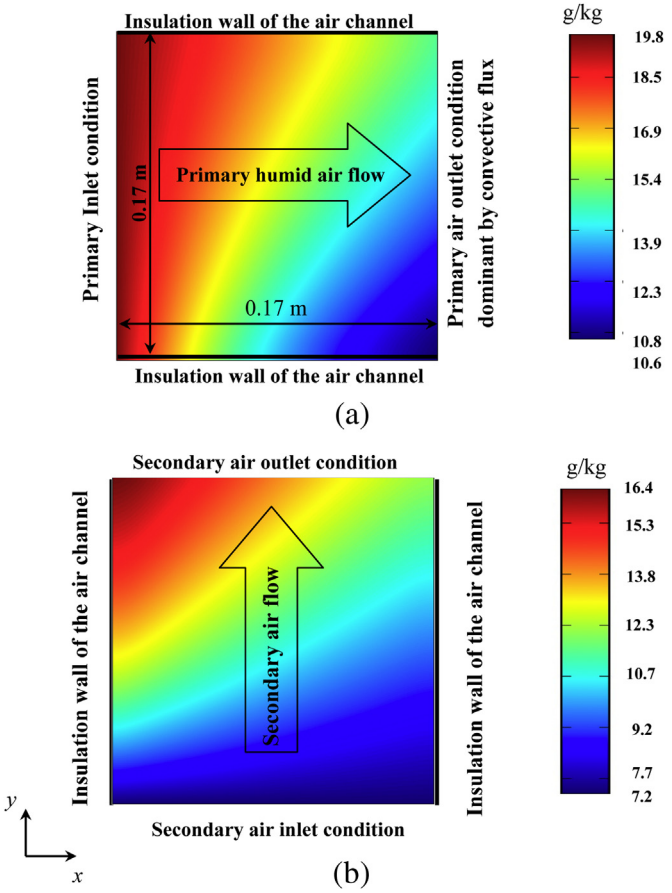

Fig. 10. COMSOL simulation results showing the moisture concentration: (a) in the primary air channel and (b) in the secondary air channel at an air flow rate of 50 m^3/h or at a specific air flow rate of 0.006 m/s, (dimension of the membranes: 17 cm length in x-direction and 17 cm width in y-direction).

where ΔQ is the latent load handled by the membrane unit, the subscript "SCC" represents "Singapore Climatic Condition" (for quantitative data see below). ΔQ_{SCC} is defined as:

$$\Delta Q_{SCC} = (\Delta\omega \times \rho \times h)_{SCC} \times A \times v, \tag{19}$$

In the analysis below ΔQ_{SCC} is evaluated for experimental conditions realised in our experiments. Using Eqs. (16) and (17), $\Delta\overline{Q}$ can be written as

$$\Delta\overline{Q} = \frac{\Delta\omega \times \dot{m} \times h}{(\Delta\omega \times \dot{m} \times h)_{SCC}} \tag{20}$$

or

$$\Delta\overline{Q} = \Delta\overline{\omega} \times \overline{v} \times \overline{h} \tag{21}$$

where $\Delta\overline{\omega} = \Delta\omega/\Delta\omega_{SCC}$ is the normalized air-dehumidification ratio of the membrane unit, $\overline{v} = v/v_{SCC}$ is the normalized specific air flow rate, $\overline{h} = h/h_{SCC}$ is the normalized specific enthalpy of water vapour:

$$\overline{h} = \frac{h_{fg} + \beta t}{h_{fg} + \beta t_{SCC}}, \tag{22}$$

$h_{fg} = 2501$ kJ/kg is the latent heat of vaporization of water at 0 °C, $\beta = 1.805$ kJ/(kg C) is the specific heat of water vapour, and t is the

Table 6
Latent load (ΔQ) handled by the membrane dehumidification unit and the normalized parameters for different experiments.

Exp no.	Ambient air temperature (°C)	Specific air flow rate ν (m/s) × 10^{-2}	ω^{P} (g/kg)	$\Delta\overline{\omega} = \frac{\Delta\omega}{\Delta\omega_{SCC}}$	ΔQ (W)	$\Delta\overline{Q} = \frac{\Delta Q}{\Delta Q_{SCC}}$
1	28.3	0.24	3	0.11	18	0.03
2	28.8	0.60	11.5	0.59	245	0.37
3	29.5	0.72	4.8	0.12	60	0.09
4	29.5	0.84	5.3	0.14	81	0.12
5	30.0	0.96	3.9	0.06	40	0.06
6	30.6	0.96	7.3	0.25	165	0.25
7	29.6	0.96	12.0	0.44	291	0.44

*ΔQ_{SCC} stands for the full latent loads by an air-conditioning unit in Singapore climatic condition.
#$\Delta\omega_{SCC}$ stands for the reference amount of moisture removal from the ambient under Singapore climatic condition.
Note: The humidity ratios of air stream of the above mentioned experiments can be found in Table 4.

air temperature in Celsius. For the normalization in our analysis, the Singapore ambient air condition are stipulated as follows: ambient air temperature $t_{SCC} = 32^{\circ\circ}$C, relative humidity 65%, and a moisture amount of 20 g/kg. Thus $\Delta\omega_{SCC} = 10$ g/kg has to be removed from the air in order to reach a supply air of 50% relative humidity at a temperature of 25 °C. Due to the limitation of the experimental set-up, the maximum air flow of our experiment is of $\dot{V}_{SCC} = 80\ m^3/h$; $\Delta\overline{Q}$ is given by the normalized air dehumidification ratio, the normalized specific air flow rate and the normalized specific enthalpy. Table 6 shows exemplary numerical results for the reduction of latent loads under Singapore climatic conditions and the specific flow rates used in our experiments (the results shown were derived from the experiments summarised in Table 4; the temperature of the primary air was about 30 °C). As can be seen from Table 6, the ambient latent load handled by membrane unit is directly influenced by the air flow rate and the dehumidification potential. These data may be useful for the assessment of the normalized latent load that can be handled by a membrane dehumidification unit under tropical conditions and thus for the design of membrane units for the given environmental condition.

The total electricity consumption of the membrane unit is determined by the electricity consumption of the air fans/blowers. This is assessed as

$$P_{ele} = \frac{\Delta p \times \dot{V}}{\xi_{fan}} \tag{23}$$

where P_{ele} is electricity consumption of the fans in W, Δp is the measured total pressure drop of the primary and secondary air streams through the membrane unit in Pa, $\dot{V}$ is volumetric air flow rate in m^3/s, and ξ_{fan} is assumed efficiency of air fan. Assuming a fan efficiency of 90%, the total electricity consumption of the two fans for primary and secondary air stream is calculated for experiment 7 (see Tables 4 and 6) as 33.3 W (see Table 7).

This required total electricity consumption of the fans of the membrane unit may be compared to the latent load reduction (enthalpy difference) of approximately 290 W. The relatively low electricity demand is due to the fact that the membrane dehumidification is driven by the difference in the moisture content of the secondary and the primary air streams.

Table 7
Electricity consumption (for latent load removal) of the membrane unit.

Exp no.	Air flow (m^3/h)	Primary air stream pressure drop (Pa)	Secondary air stream pressure drop (Pa)	Assumed fan efficiency (−)	Electricity consumption of fans (W)	ΔQ (W)
7	80	730	620	0.9	33.3	291

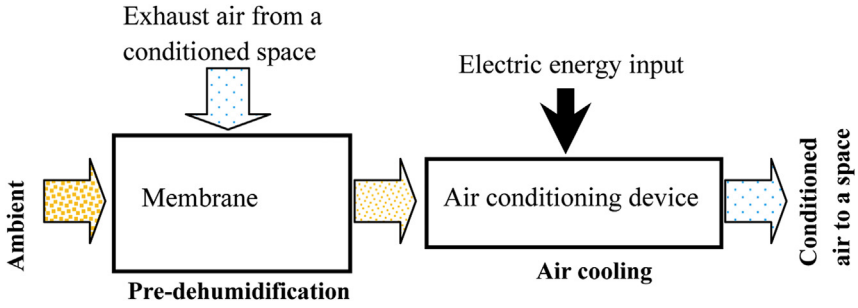

Fig. 11. A membrane dehumidification unit in combination with a conventional air cooling device.

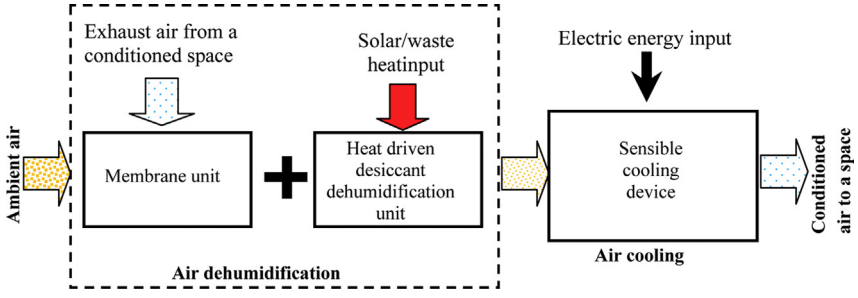

Fig. 12. A two-stage dehumidification system integrated with a sensible cooling device.

5. Potential applications of membrane dehumidification units in air conditioning systems

According to the results of this paper, the membrane technology has a considerable potential for air dehumidification in air-conditioning applications. Membrane dehumidification units could be implemented, e.g., in following scenarios:

- Scenario-1 is a single stage membrane air dehumidification combined with a (highly efficient) conventional cooling device (see Fig. 11), resulting in electricity saving due to the fact that the latent load is handled by the membrane unit. Please note that a relatively dry air from an air-conditioned space (exhaust air) is necessary for the operation of a membrane based air dehumidification unit. The air cooling unit could handle a residual latent load as well. This scheme seems to be favourable for air conditioning in medium humidity climates.
- Scenario-2 consists of a multi-stage air dehumidification in combination with a (highly efficient) conventional sensible cooling device. The membrane unit can be implemented as a pre-dehumidification device in particular in tropical climates. As illustrated in Fig. 12, latent loads are handled by a two-stage dehumidification system – a membrane pre-dehumidifier and a secondary complementary air dehumidifier, e.g., a desiccant based air dehumidifier. The dehumidified air is subsequently cooled by an electricity powered sensible cooling device. This device can operate at an elevated evaporator temperature of about 16–20 °C since only the sensible load has to be covered. Whereas, conventional air-conditioning systems in the tropics have to operate at lower temperatures of about 5–10 °C in order to dehumidify the air sufficiently. The handling of the latent loads by the two-stage dehumidification unit and the elevated operation temperature of the cooling device will result in a considerable electricity saving. On the other hand, it is noted that a thermal energy source (at a temperature around 80 °C) is necessary for the regeneration of the water absorber if e.g. a desiccant air dehumidification system is deployed. The operation of such a system could result in higher electricity savings compared to the scenario-1, in particular in the tropics as the total latent load is handled by the multi-stage air dehumidifier. Therefore, a highly efficient use of electricity can be expected, but the installation of such systems may be more complex and costly.

6. Conclusions

A simple electricity efficient air dehumidification unit has been analysed under tropical conditions. Membrane dehumidification units using nonsophisticated membranes have the potential to significantly reduce the water content of ambient air in air-conditioning applications. The process of dehumidification is driven by the gradient of the concentration of water vapour between the incoming ambient air and the relatively dry exhaust air from a building; electric energy is only used to for air transport (blowers). Experiments have demonstrated a moisture reduction of up to 8 g per kg of dry air for humid ambient air having a moisture content of 20 g per kg of dry air. This number applies to a flow rate of 20 m^3/h and a membrane area of 2.3 m^2 while the dry exhaust air from a building had a moisture content of 7–8 g/kg. The experimental results presented in the paper show that the moisture removal potential of the membrane unit highly depends on the air flow rate and the humidity of the relatively dry exhausts air form a building which is driving the dehumidification process. Combining membrane air dehumidification units with other air dehumidification devices (e.g., desiccant based air dehumidifiers) may be in particular suited for the tropics or high humidity climates.

Acknowledgements

The authors would like to thank to the solar-assisted air conditioning team at SERIS and the Clean Energy Research Program Office (CEPO), Singapore for the financial support during the course of this work.

Nomenclature

A	total area of membrane (m^2)
c	water vapour concentration (kg/m^3)
D	mass diffusion coefficient (m^2/s)
D	parameter domain of diffusion coefficient
h	specific enthalpy for saturated water vapour (kJ/kg)
h_{fg}	latent heat of vaporization at 0 °C (kJ/kg)
$\overline{h}$	normalized specific enthalpy for saturated water vapour (–)
H	height of primary/secondary channels and thickness of membrane
S	specific moisture flux rate across the membrane surface (kg/m^2 s)
k	convective mass transfer coefficient (m/s)
L	characteristic length (m)
$\dot{m}$	primary air flow rate (kg/s)
P	air pressure (Pa)
P_{ele}	electricity consumption of fan (W)
Q	latent load handled (W)
$\overline{Q}$	normalized latent load (–)
Re	Reynolds number (–)
Sc	Schmidt number (–)
Sh	Sherwood number (–)
t	air temperature in degree Celsius (°C)
$\mathbf{u}$	air velocity of the air (m/s)
$\dot{V}$	air volume flow rate (m^3/h)

Greek letters

ω	humidity ratio of primary air at the entrance of the membrane unit (g/kg)
ω^P	dehumidification potential (g/kg)
$\Delta\omega$	the amount of moisture removed between primary and secondary air streams (g/kg)
$\Delta\overline{\omega}$	normalized air dehumidification ratio of the membrane unit
η	latent effectiveness (–)
α_i	coefficients determined by a multi regression analyses (–)
e	error between computed and measured data of humidity ratios (%)
μ	dynamic viscosity of air (kg m^{-1} s^{-1})
ρ	density of air (kg/m^3)
β	specific heat of water vapour (kJ kg^{-1} C^{-1})
v	specific air flow rate (m/s)
$\overline{v}$	Normalized specific air flow rate (–)
ξ	efficiency of fan

Subscripts

ele	electricity
in	inlet condition of air stream
m	membrane, membrane side
out	outlet condition of air stream
p	primary air stream, primary air side

s secondary air stream, secondary air side
SCC Singapore Climatic Condition

References

[1] M. Suzuki, Adsorption Engineering, Kodansha Ltd, Tokyo and Elsevier Science Publishers B. V., Amsterdam, 1990.
[2] Hans-Martin Henning, Solar-assisted Air Conditioning in Buildings, Springer Wien, New York, 2004, ISBN 3-211-00647-8.
[3] G. Angrisani, C. Roselli, M. Sasso, Experimental validation of constant efficiency models for the subsystems of an unconventional desiccant-based air handling unit and investigation of its performance, Applied Thermal Engineering 33–34 (2012) 100–108.
[4] G. Panaras, E. Mathioulakis, V. Belessiotis, N. Kyriakis, Theoretical and experimental investigation of the performance of a desiccant air-conditioning system, Renewable Energy 35 (7) (2010) 1368–1375.
[5] R.D. Noble, S.A. Stern, Membrane Separations Technology, Principles and Applications, Elsevier Science B.V., Amsterdam, The Netherlands, 1995.
[6] M. Khayet, Membrane and theoretical modeling of membrane distillation: a review, Advances in Colloid and Interface Science 164 (2011) 56–88.
[7] B.L. Pangarkar, M.G. Sane, M. Guddad, Reverse osmosis and membrane distillation for desalination of groundwater: A review, ISRN Materials Science (2011), http://dx.doi.org/10.5402/2011/523124.
[8] D. Agro, Wastewater reclamation by reverse osmosis, Journal WPCF 51 (1979) 590.
[9] J.-H. Wee, Application of proton exchange membrane fuel cell systems, Renewable and Sustainable Energy Reviews 11 (2007) 1720–1738.
[10] F. Liu, B. Yi, D. Xing, J. Yu, H. Zhang, Nafion/PTFE composite membranes for fuel cell applications, Journal of Membrane Science 212 (2003) 213–223.
[11] M. Tomaszewska, M. Gryta, A.W. Morawski, Mass transfer of HCL and H_2O across the hydrophobic membrane during membrane distillation, Journal of Membrane Science 166 (2000) 149–157.
[12] J.L. Niu, L.Z. Zhang, Membrane-based enthalpy exchanger: material considerations and clarification of moisture resistance, Journal of Membrane Science 189 (2001) 179–191.
[13] L.Z. Zhang, Y. Jiang, Heat and mass transfer in a membrane-based energy recovery ventilator, Journal of Membrane Science 163 (1999) 19–38.
[14] L.Z. Zhang, J.L. Niu, Effective correlations for heat and moisture transfer processes in an enthalpy exchanger with membrane cores, Journal of Heat Transfer 124 (2009) 922–929.
[15] L.Z. Zhang, Heat and mass transfer in plate-fin enthalpy exchangers with different plate and fin materials, International Journal of Heat and Mass Transfer 52 (2009) 2704–2713.
[16] P. Scovazzo, A. Hoehn, P. Todd, Membrane porosity and hydrophilic membrane-based dehumidification performance, Journal of Membrane Science 167 (2000) 217–225.
[17] S. Liu, S. Riggat, X. Zhao, Y. Yuan, Impact of adsorbent finishing and absorbent filming on energy exchange efficiency of an air-to-air cellulose fibre heat and mass exchanger, Building and Environment 44 (2009) 1803–1809.
[18] A. Ito, Dehumidification of air by a hygroscopic liquid membrane support on surface of a hydrophobic microporous membrane, Journal of Membrane Science 175 (2000) 35–42.
[19] ASHRAE Handbook, 1997 Fundamentals, Chapter 6 Psychrometrics (1997).
[20] L.Z. Zhang, Mass diffusion in a hydrophobic membrane humidification/dehumidification process: the effects of membrane characteristics, Separation Science and Technology 41 (2006) 1565–1582.
[21] ASHRAE Handbook, 1997 Fundamentals, Chapter 5 Mass Transfer (1997).
[22] ASHRAE Handbook, 1997 Fundamentals, Chapter 3 Heat Transfer (1997).
[23] O.C. Zienkiewicz, The Finite Element Method, fourth ed., McGraw-Hill, London, 1989.
[24] L.Z. Zhang, Evaluation of moisture diffusivity in hydrophilic polymer membranes: a new approach, Journal of Membrane Science 269 (2006) 75–83.
[25] P.R. Bevington, D.K. Robinson, Data Reduction and Error Analysis for the Physical Sciences, McGraw-Hill, New York, 1992.